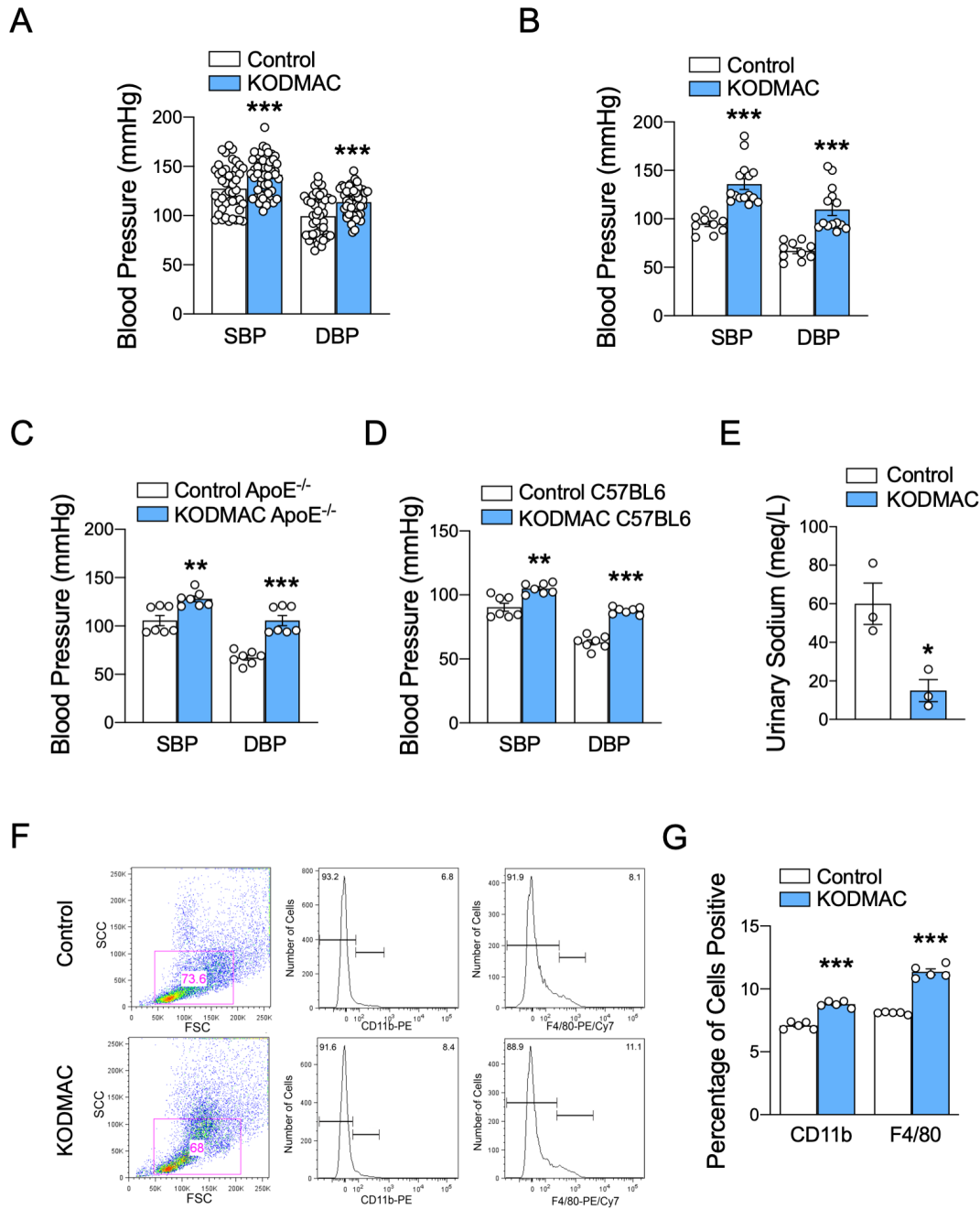


Supplementary Information

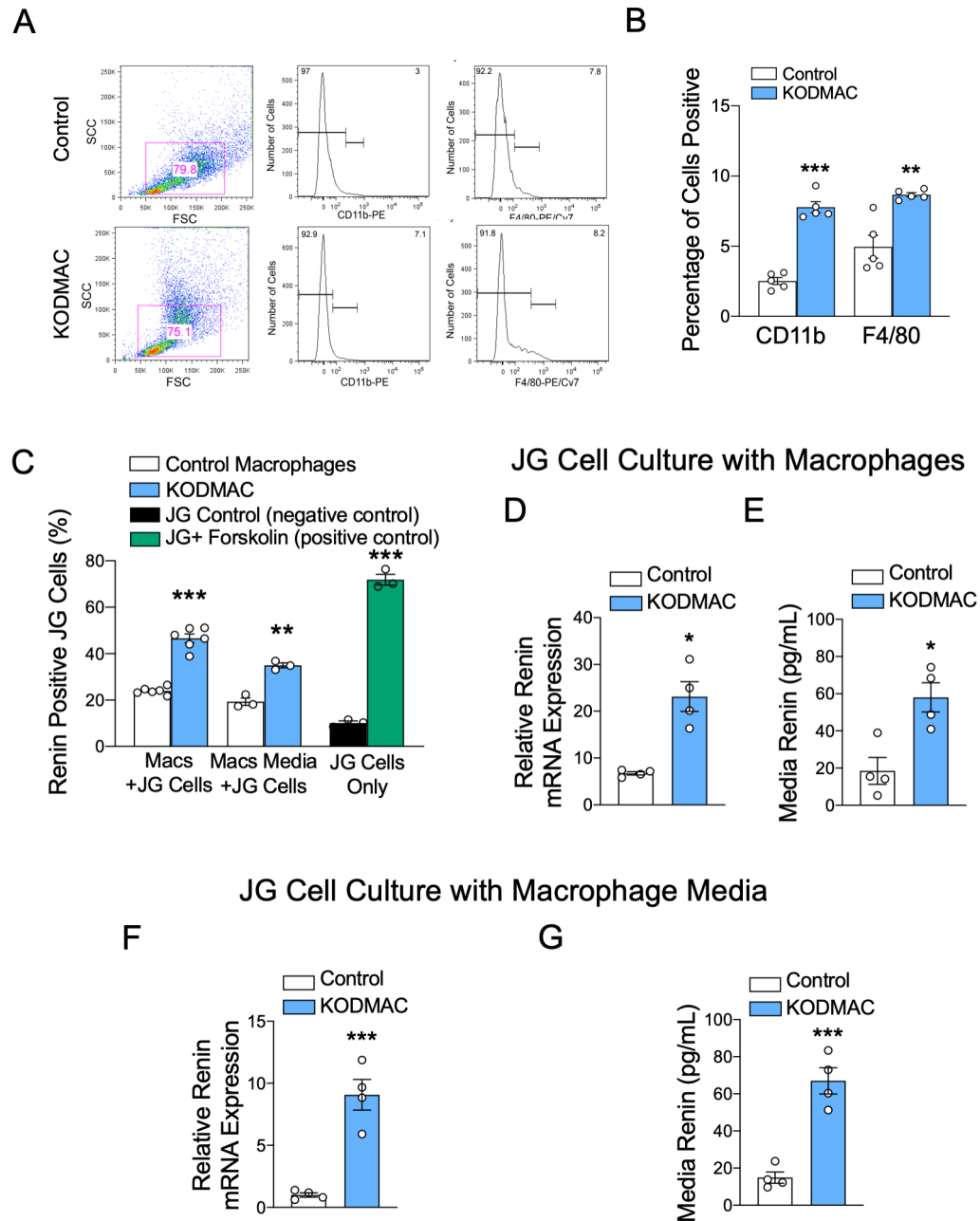
Macrophage Secretion of miR-106b-5p Causes Renin-Dependent Hypertension

J. Oh, S.J. Matkovich, A.E. Riek, S.M. Bindom, J.S. Shao, R.D. Head, R.A. Barve, M.S. Sands, Geert Carmeliet, P. Osei-Owusu, R.H. Knutsen, H. Zhang, K.J. Blumer, C.G. Nichols, R.P. Mecham, A. Baldan, B.A. Benitez, M.L. Sequeira-Lopez, R.A. Gomez, and C. Bernal-Mizrachi

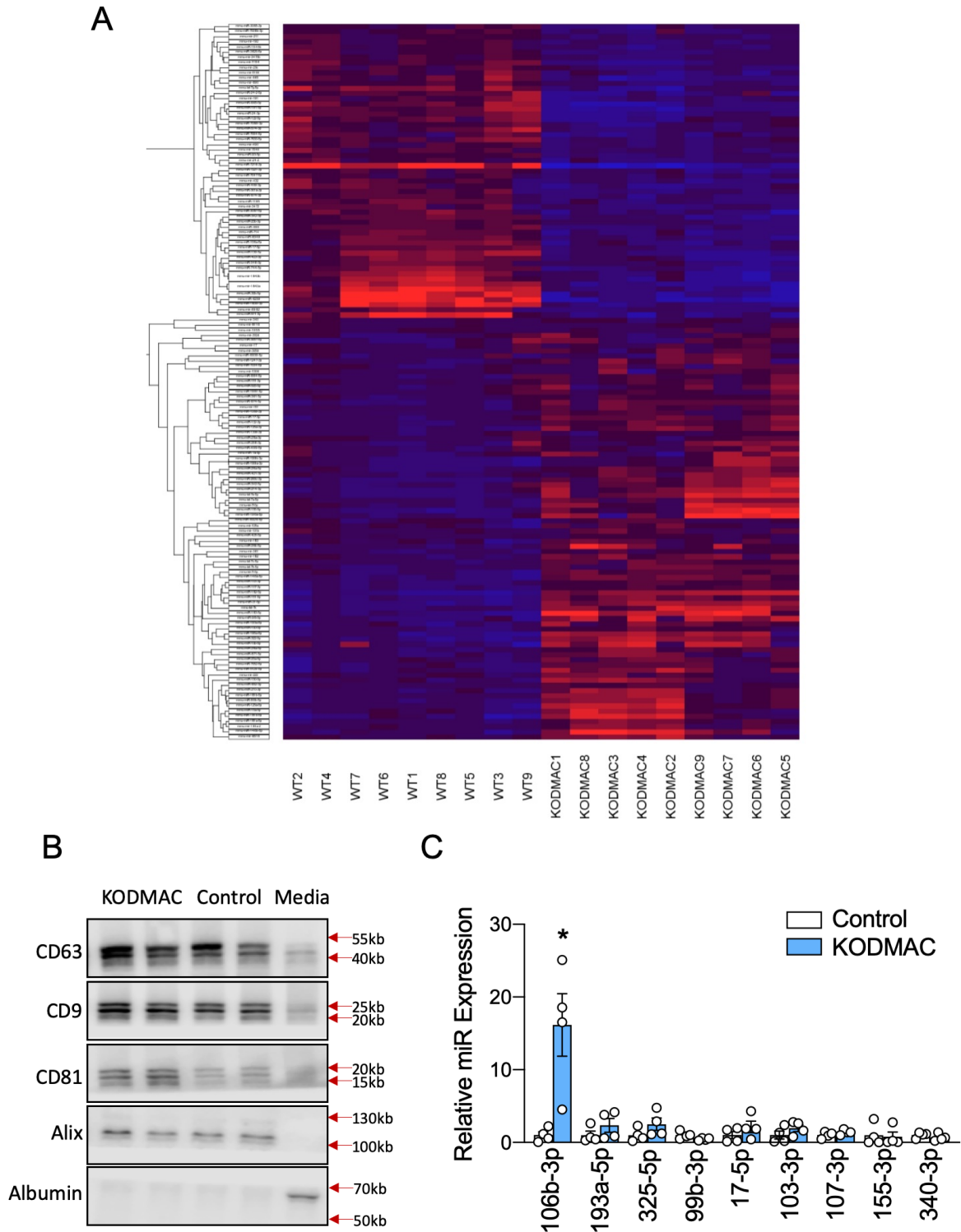
Supplementary Figures and Figure Legends



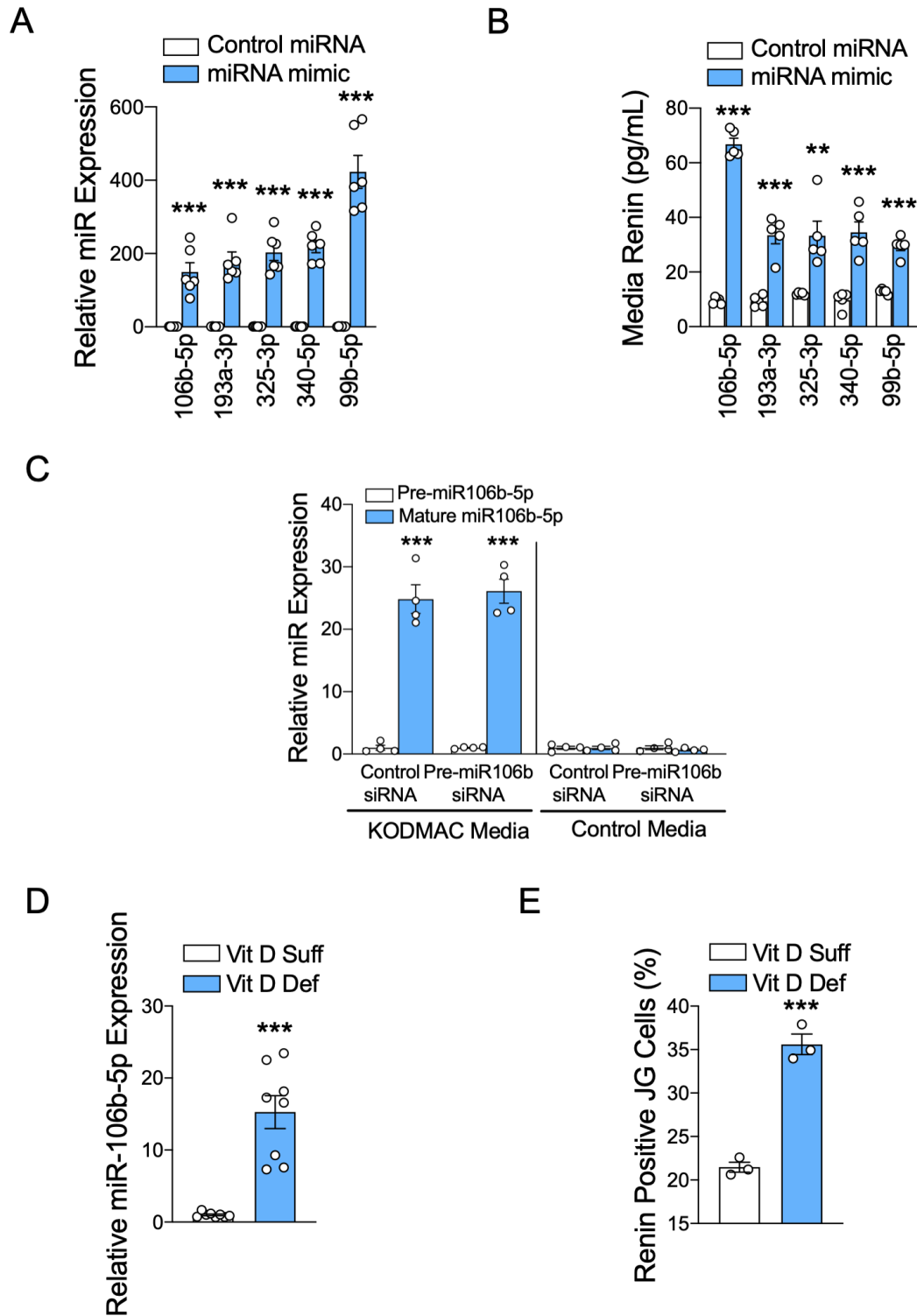
Supplementary Figure 1. Myeloid *Vdr* deletion induces persistent high blood pressure by renin activation in multiple mouse backgrounds. Non-invasive SBP and DBP in KODMAC or control mice at **(A)** 8 weeks old (n=52 KODMAC/45 control) and **(B)** 1 year old (n=15 KODMAC/11 control) in the LDLR^{-/-} background. Non-invasive blood pressure in 8-week-old mice with deletion of *Vdr* in macrophages in the **(C)** ApoE^{-/-} (n=7/group) or **(D)** C56BL-6 backgrounds (n=7/group). In 8-week-old KODMAC or control mice: **(E)** urinary sodium (n=3/group) and flow cytometry **(F)** Cell aggregates, dead, and cellular debris were excluded based on FSC/SCC. Batch analysis by FlowJo was used for gating consistency. Isotype control for anti-CD11b PE and F4/80 PE-Cy7 respectively were used to ensure antibody specific binding and **(G)** quantification of CD11b and F4/80 macrophage marker positivity of dissected aortas. (n=5/group). Data expressed as mean ± SEM from student's two-tailed unpaired *t* test with **p*<0.05, ***p*<0.01, ****p*<0.001 vs. control.



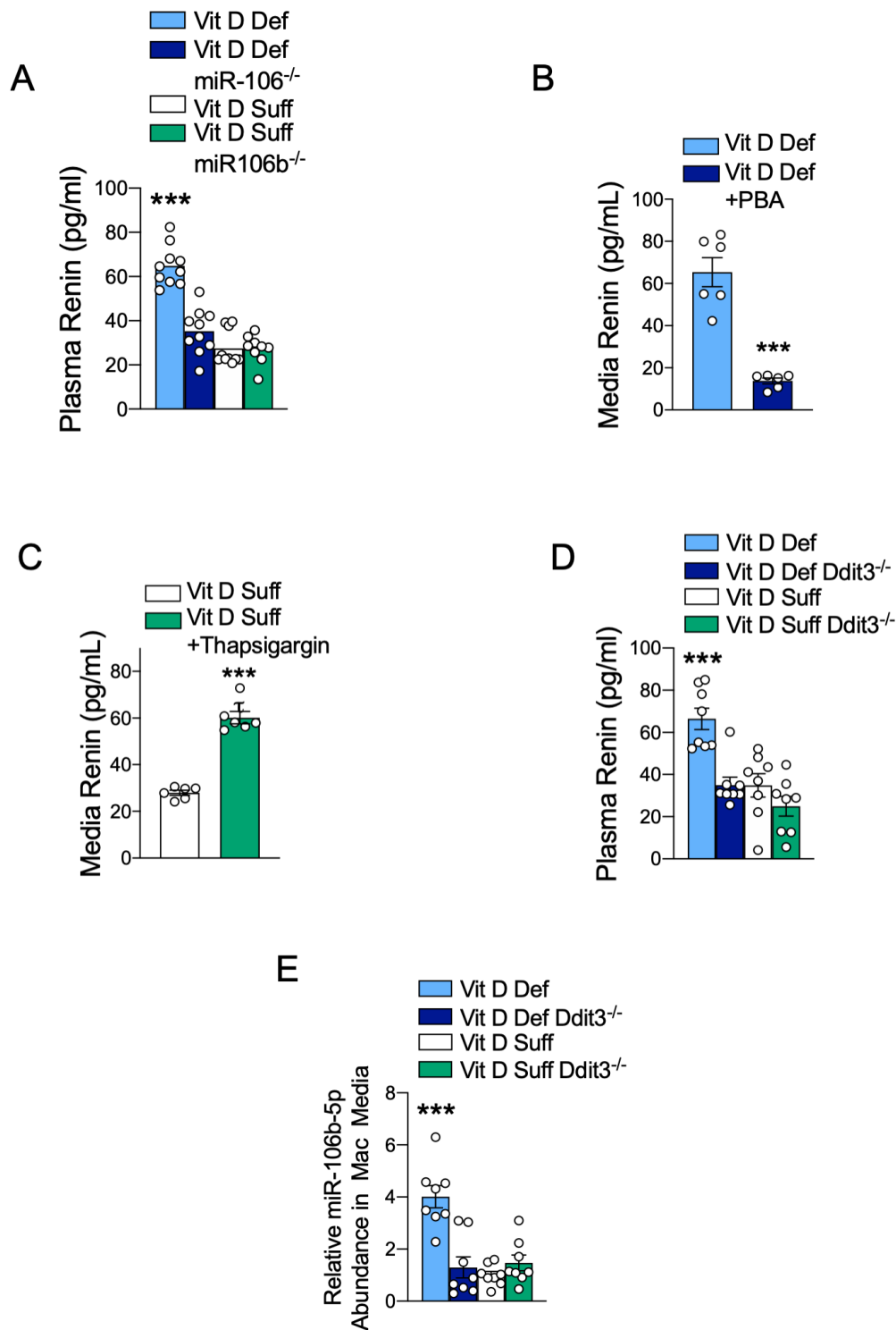
Supplementary Figure 2. KODMAC macrophages or macrophage media induce JG cell renin production. Flow cytometry (A) Cell aggregates, dead, and cellular debris were excluded based on FSC/SCC. Batch analysis by FlowJo was used for gating consistency. Isotype control for anti-CD11b PE and F4/80 PE-Cy7 respectively were used to ensure antibody specific binding and (B) quantification of CD11b and F4/80 macrophage marker positivity of homogenized kidney (n=5/group). (C) Renin-positive (YFP-labeled Ren^{1c}) JG cells by immunofluorescence microscopy after co-culture with KODMAC or control macrophages (n= 6/group) or their media (n=3/group) with JG cells only as negative control and Forskolin as positive control. (D) RT-qPCR of relative renin mRNA abundance in JG cells or (E) media renin after JG cell co-culture with KODMAC or control macrophages (n=4/group). (F) RT-qPCR of relative renin mRNA abundance in JG cells or (G) media renin after JG cell culture with KODMAC or control macrophage media (n=4/group). Data expressed as mean \pm SEM from student's two-tailed unpaired *t* test with **p*<0.05, ***p*<0.01, ****p*<0.001 vs. control.



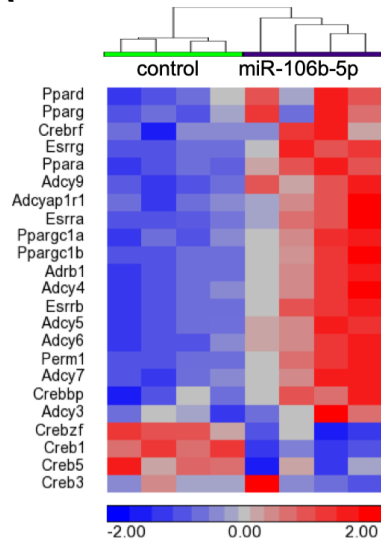
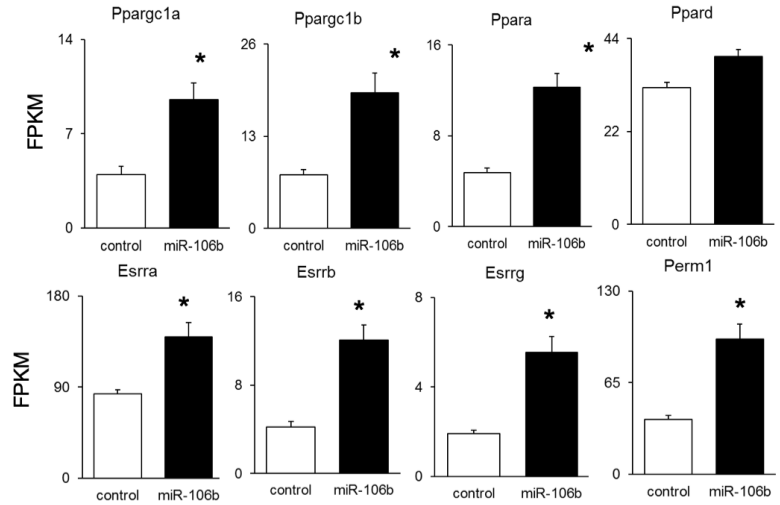
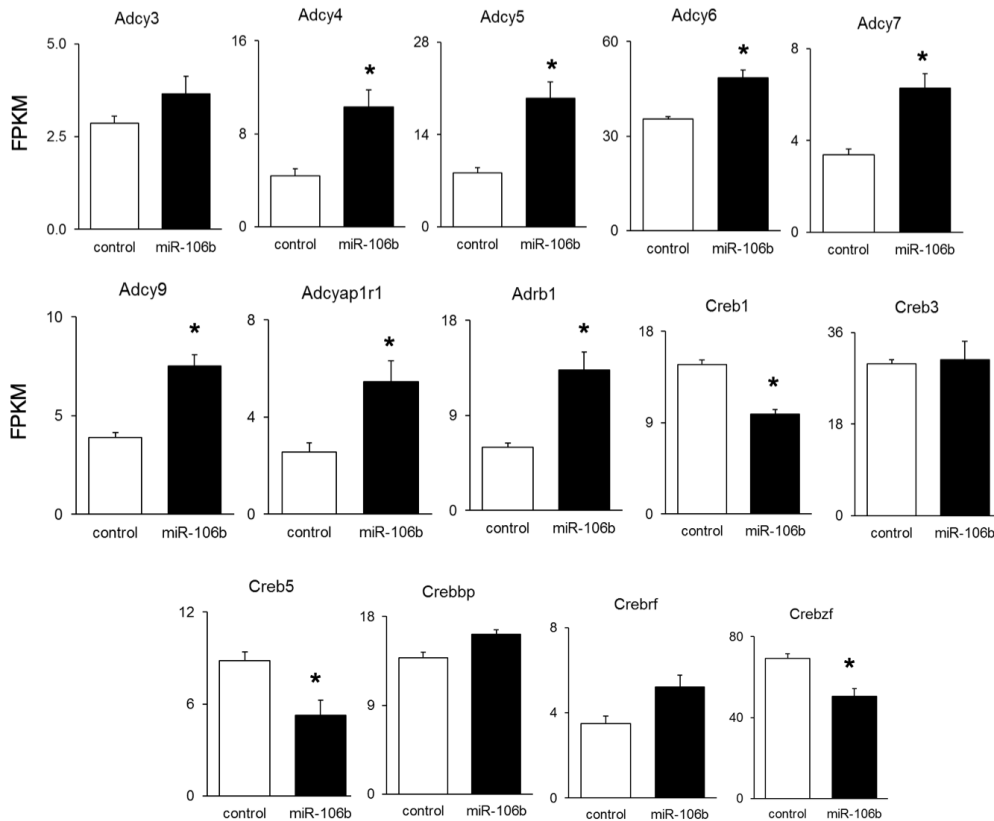
Supplementary Figure 3. KODMAC macrophages demonstrate differentially abundant miRNAs in macrophage media compared to control. (A) Standardized heatmap depicting alterations in miRNAs differentially abundant ($p < 0.05$) in the media of KODMAC vs. control macrophages ($n=9/\text{group}$). (B) Exosome protein expression in media from KODMAC, control or exosome-free media (representative of 2/group); (C) Relative miRNA expression (less abundant 5p or 3p species) from KODMAC or control peritoneal macrophage media exosomes ($n=4/\text{group}$). Data expressed as mean \pm SEM from student's two-tailed unpaired t test with $*p < 0.05$ vs. control.



Supplementary Figure 4. Vitamin D deficiency induces macrophage miR-106b-5p secretion and JG cell renin production. (A) RT-qPCR of relative miR abundance in JG cells after transfection with miR-mimic or control (n=6/group). (B) Media renin after JG cell transfection with miR-mimic or control (n=5/group). (C) Relative abundance of pre-miR-106b-5p and mature miR-106b-5p in JG cells after transfection with pre-miR-106b siRNA (to suppress endogenous miR-106b-5p production) or control siRNA and exposure to KODMAC or control macrophage media (n=4/group). After co-culture with media from macrophages of vitamin D-deficient vs. sufficient mice: (D) RT-qPCR of relative miR-106b-5p abundance in JG cells (n=8/group) and (E) renin-positive (YFP-labeled Ren^{1c}) JG cells by immunofluorescence microscopy (n=3/group). Data expressed as mean ± SEM from student's two-tailed unpaired *t* test with ***p<0.001 vs. (A-B) control, (C) pre-miR-106b-5p, or (D-E) vitamin D sufficient.



Supplementary Figure 5. Vitamin D deficiency induces macrophage miR-106b-5p secretion and JG cell renin production. (A) Plasma renin in *miR106b*^{-/-} or control mice fed vitamin D-deficient and –sufficient diets (n=5/group). (B) media renin of JG cells co-cultured with media from vitamin D-deficient peritoneal macrophages treated with or without phenylbutyric acid (PBA) (n=6/group). (C) Media renin from media of JG cells co-cultured with media from vitamin D-sufficient peritoneal macrophages treated with or without Thapsigargin (n=6/group). (D) Plasma renin (E) miR106b abundance in macrophage media in *Ddit3*^{-/-} or control mice fed vitamin D-deficient and –sufficient diets (n=8/group). Data expressed as mean ± SEM from (A,D,E) one-way ANOVA with Tukey’s post hoc test with ***p<0.001 vs. all and (B,C) student’s two-tailed unpaired *t* test with ***p<0.001 vs. vitamin D deficient or sufficient control.

A**B****PPAR-related****C****CREB-related**

* FDR<0.01

Supplementary Figure 6. miR-106b-5p transfection into JG cells modulates PPAR and CREB signaling mRNAs. (A) Global mRNA alterations for key PPAR and CREB signaling genes by RNA-sequencing of miR-106b-transfected JG cells (red=higher expression; n=4/group). (B) PPAR (C) CREB-related mRNA abundance (expressed as FPKM) from global polyA-RNA sequencing from JG cells after transfection with miR-106b-5p mimic or control (n=4/group). Data expressed as mean \pm SEM from student's two-tailed unpaired *t* test with **p*<0.05 vs. control.

Human E2F1

Position 387-393 of E2F1 3' UTR

[hsa-miR-106b-5p](#)

Position 980-986 of E2F1 3' UTR

[hsa-miR-106b-5p](#)

Mouse E2f1

Position 470-476 of E2f1 3' UTR

[mmu-miR-106b-5p](#)

Position 985-991 of E2f1 3' UTR

[mmu-miR-106b-5p](#)

Human PDE3B

Position 172-178 of PDE3B 3' UTR

[hsa-miR-106b-5p](#)

Mouse Pde3b

Position 151-157 of Pde3b 3' UTR

[mmu-miR-106b-5p](#)

TargetScan 7.1

5' ...GGGGGGGCUCUAACUGCACUUUC...

| | | | | | | | | | |
3' UAGACGUGACAGUCGUGAAA

5' ...CCCACCCUCCAAUCUGCACUUUG...

| | | | | | | | | | |
3' UAGACGUGACAGUCGUGAAA

5' ...GGGUGGGCUCUAACUGCACUUUU...

| | | | | | | | | | |
3' UAGACGUGACAGUCGUGAAA

5' ...CCCACCCUCCAGUCUGCACUUUG...

| | | | | | | | | | |
3' UAGACGUGACAGUCGUGAAA

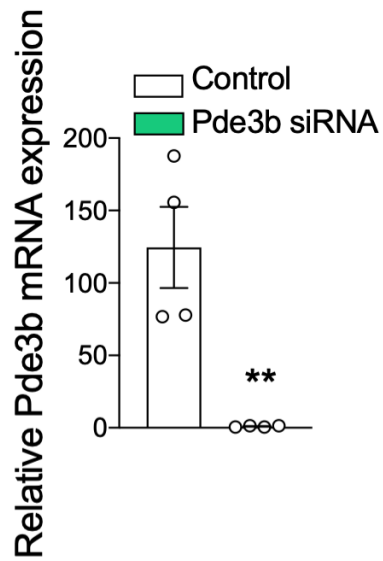
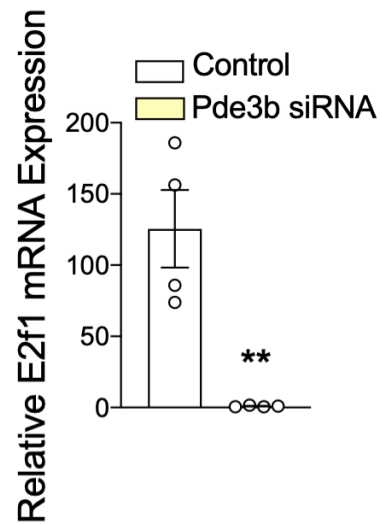
5' ...GUUUCCACUCCUAUGCACUUUC...

| | | | | | | | | | | |
3' UAGACGUGACAGU-CGUGAAA

5' ...AGUUCUCACUCCUAAGCACUUUC...

| | | | | | | | | | | | |
3' UAGACGUGACAGU-CGUGAAA

Supplementary Figure 7. TargetScan7.1 predictions of miR-106b-5p binding sites in 3' UTRs of both mouse and human E2f1 and Pde3b.

A**B**

Supplementary Figure 8. Pde3b and E2f1 siRNA knockdown in JG cells suppresses mRNA expression. RT-qPCR analysis of relative (A) Pde3b and (B) E2f1 mRNA expression in JG cells after transfection with Pde3b or E2f1 siRNA (n=4/group). Data expressed as mean ± SEM from student's two-tailed unpaired *t* test with ***p*<0.01 vs. control.